

ARTICLE

Seasonal Remote-Sensing Observations of Aerosol-Cloud Relationships under Varied Water Vapor Conditions

Stavros Stathopoulos *[✉], Konstantinos Kourtidis, Alexandra Gemitzi

Laboratory of Atmospheric Pollution and Pollution Control Engineering of Atmospheric Pollutants, School of Engineering, Democritus University of Thrace, Xanthi 67100, Greece

ABSTRACT

Understanding the aerosol-cloud relationship is critical for reducing uncertainties in climate projections, especially over regions that experience complex aerosol dynamics from both natural and anthropogenic sources. This study aims to investigate how aerosols influence cloud properties under varying water vapor conditions over nine urban and rural subregions of the Eastern Mediterranean, disentangling the seasonal and annual relationships between aerosols and cloud parameters while distinguishing the effects of different aerosol types. For this purpose, Aerosol Optical Depth (AOD) at 550 nm, Water Vapor (WV) under clear-sky conditions, Cloud Cover (CC), Cloud Optical Depth (COD), and Cloud Top Pressure (CTP) from the Moderate Resolution Imaging Spectroradiometer (MODIS) sensor onboard the Aqua satellite, for the time period July 2002–December 2012. Additionally, anthropogenic (AOD_{anthr}) and dust AOD (AOD_{dust}) datasets, constructed through a synergy of satellite observations, chemical transport modeling, and reanalysis products were utilised. Our results reveal consistent increases in CC with increasing total, anthropogenic, and dust aerosol loading across all regions, seasons, and water vapor levels, supporting the hypothesis of aerosol-induced cloud invigoration. COD was found to increase with AOD when AOD < 0.5 but remain steady or decline for higher AOD levels, independent of water vapor concentration. Furthermore, anthropogenic aerosols tend to enhance COD more strongly than dust aerosols. Seasonal differences in cloud height were also observed: in spring and summer, CTP decreases (indicating higher cloud tops) with increasing AOD and CC, while in autumn and winter, under high water vapor conditions, aerosol loading leads to higher

***CORRESPONDING AUTHOR:**

Stavros Stathopoulos, Laboratory of Atmospheric Pollution and Pollution Control Engineering of Atmospheric Pollutants, School of Engineering, Democritus University of Thrace, 67100 Xanthi, Greece; Email: sstathop@env.duth.gr

ARTICLE INFO

Received: 15 April 2025 | Revised: 10 July 2025 | Accepted: 17 July 2025 | Published Online: 25 July 2025
DOI: <https://doi.org/10.30564/jasr.v8i3.9528>

CITATION

Stathopoulos, S., Kourtidis, K., Gemitzi, A., 2025. Seasonal Remote-Sensing Observations of Aerosol-Cloud Relationships under Varied Water Vapor Conditions. *Journal of Atmospheric Science Research*. 8(3): 97–114. DOI: <https://doi.org/10.30564/jasr.v8i3.9528>

COPYRIGHT

Copyright © 2025 by the author(s). Published by Bilingual Publishing Group. This is an open access article under the Creative Commons Attribution-NonCommercial 4.0 International (CC BY-NC 4.0) License (<https://creativecommons.org/licenses/by-nc/4.0/>).

clouds.

Keywords: Aerosols; Clouds; Water Vapor; Eastern Mediterranean; Cloud Height

1. Introduction

The intricate impact of aerosols on climate has drawn the attention of the scientific community for decades, stimulating efforts to disentangle their role in climate change^[1–4]. Aerosols can modify cloud properties by acting as cloud condensation nuclei (CCN), leading to smaller and more numerous cloud droplets, increasing cloud albedo, a process known as “first aerosol indirect effect” or “Twomey effect”^[5]. These cloud droplets may delay the onset of collision and coalescence inside the cloud, inhibiting precipitation and increasing their lifetime, a process known as “second indirect effect”^[6]. Furthermore, aerosols have been observed to absorb and scatter radiation, a phenomenon referred to as the “aerosol direct effect.” The presence of absorbing aerosols has been demonstrated to have a significant impact on atmospheric conditions. These particles can alter the thermal structure of the atmosphere, leading to an increase in water vapor evaporation, due to radiative absorption. This in turn, results in a suppression of cloud formation or a reduction in cloud density, a phenomenon referred to as the “semi-direct effect”^[7–9].

The Eastern Mediterranean Territory (EMT) is a climatically sensitive region which is strongly affected by air pollution. It is considered an ideal region to investigate the aerosol-cloud relationships primarily due to its unique aerosol composition, geographical positioning and climate sensitivity^[10–16]. The region is a crossroad of various aerosol source regions as it receives anthropogenic aerosols from Europe and the Middle East, dust from North Africa and biomass burning aerosols from southeastern Europe and Asia^[10,14]. This blend of dust, anthropogenic and biomass burning aerosols can significantly impact cloud microphysics^[17]. Anthropogenic aerosols are associated with large coastal megacities such as Cairo or Athens, showing high values of Aerosol Optical Depth (AOD) in the visible range^[11]. Hatzianastassiou et al.^[10] investigated AOD over large urban regions in the eastern Mediterranean using remote sensing data from the Total Ozone Mapping Spectrometer (TOMS) and Moderate Resolution Imaging Spectroradiometer (MODIS) instruments, finding high AOD values (up to 0.8) of anthro-

pogenic origin. In addition, Tutsak and Kocak^[18], using in situ measurements from the Aerosol Robotic Network (AERONET), found a significant presence of anthropogenic aerosols in the area. On the other hand, Balis et al.^[19] by studying the influence of biomass-burning aerosols over Thessaloniki in Greece, reported very high AOD values in the region. Furthermore, Meloni et al.^[20] and Pace et al.^[21], by investigating the optical properties of aerosols over the Mediterranean using a Multi-Filter Rotating Shadowband Radiometer (MFRSR), found that the highest biomass-burning AOD values were observed during the summer months (July–August). The high impact of biomass burning aerosols on the region has also been noted by Methymaki et al.^[22], who investigated their effect on light absorption and cloud cover using the Weather Research and Forecasting (WRF)-Chem model. In another research, Kalivitis et al.^[23] investigated the transport of dust aerosols over the EMT using data from TOMS, AERONET, and ground measurements, finding that high concentrations are transported during autumn and spring. In addition, the EMT is considered as a climate change hotspot due to its strong radiative responses to aerosol forcing^[16], while its distinctive morphology further increases the region’s sensitivity to aerosol perturbations^[21].

The aforementioned researches investigate the spatiotemporal variability of different aerosol types and the relations between aerosols and clouds without considering the different water vapor conditions over the area, as water vapor plays a pivotal role in aerosol-cloud interactions^[2,24]. The aim of this paper is to investigate the annual and seasonal relationships of different aerosol types with cloud parameters under different water vapor conditions, utilizing data from the MODIS instrument onboard the Aqua satellite, in order to enhance our understanding of aerosol-cloud interactions over the region.

2. Study Area, Materials and Methods

To study the aerosol-cloud relationships over the Eastern Mediterranean Territory (EMT) (30°–5° N,

17.5°–37.5° E), we divided the whole region into nine rural-urban subregions. Particularly, we separated the EMT into the Northern Balkans Land region (NBL) (42.3°–45° N, 17.5°–37.5° E), the Southern Balkans region (SBL) (34.4°–42.3° N, 17.5°–29.2° E), the Anatolia Land region (ANL) (34°–42.3° N, 29.2°–37.5° E), the Northern Africa Land region (NAL) (30°–34° N, 17.5°–37.5° E), the Black Sea Oceanic region (BSO) (40°–45° N, 27°–37.5° E), the Northwestern Oceanic region (NWO) (34.4°–45° N, 17.5°–27° E), the Southwestern Oceanic region (SWO) (30°–34.4° N, 17.5°–27° E), the Northeastern Oceanic region (NEO) (34.4°–40° N, 27°–37.5° E) and the Southeastern Oceanic region (SEO) (30°–34.4° N, 27°–37.5° E) (**Figure 1**). The separation was made using geographical, land type and land use criteria, following Georgoulias et al. [14]. Air quality in these regions is impacted not only from anthropogenic activities (biomass burning, traffic, heavy industry etc.) but also from sea salt emissions and the transport of dust from nearby deserts. For example, BSO is heavily impacted from biomass burning aerosols transported from Russia and Eastern Europe [25], while NAL and ANL suffer from high dust concentrations from local sources and nearby deserts [14]. In order to generalize our results over the nine subregions, we considered two broader regions to encompass all the land and oceanic areas separately, namely the Eastern Mediterranean Land (EML) and Eastern Mediterranean Oceanic (EMO) regions, respectively. EML region

comprises of the NBL, SBL, ANL and ANL regions, while EMO region includes the BSO, NWO, SWO, NEO and SEO regions. Here, we present the results for EMT, EMO and EML regions only, since the aerosol-cloud relationships over each sub-region were found to exhibit similar behaviour to that of the larger region to which it belongs.

The MODIS sensor, onboard Aqua satellite (launched in early 2002), measures the reflected terrestrial radiation and solar radiance in 36 spectral bands with a spatial resolution between 250 m and 1 km, from a height of approximately 700 km. Having a swath of about 2300 km, it nearly covers the entire globe daily [26]. Aqua satellite passes over the region twice a day, in daytime (13:30 LST) (Local Standard Time) and at nighttime (01:30 LST). The MODIS retrieval algorithm makes use of three different aerosol algorithms, measuring the aerosol scattered radiation, using visible and near-infrared channel measurements. Over land, the Dark Target (DT) algorithm chooses from a set of fine-made dominated aerosol models and a single coarse-made dominated aerosol model [27–29], while over bright land surfaces the Deep Blue (DB) algorithm has been widely used instead [30]. The third algorithm is used over oceanic regions [29,31]. The cloud parameters (cloud cover, cloud optical depth, cloud top pressure) and water vapor from MODIS, are derived using different retrieval algorithms. Details about the calculation and derivation of the MODIS products can be found in Ackerman et al. [32], King et al. [33] and Platnick et al. [34].

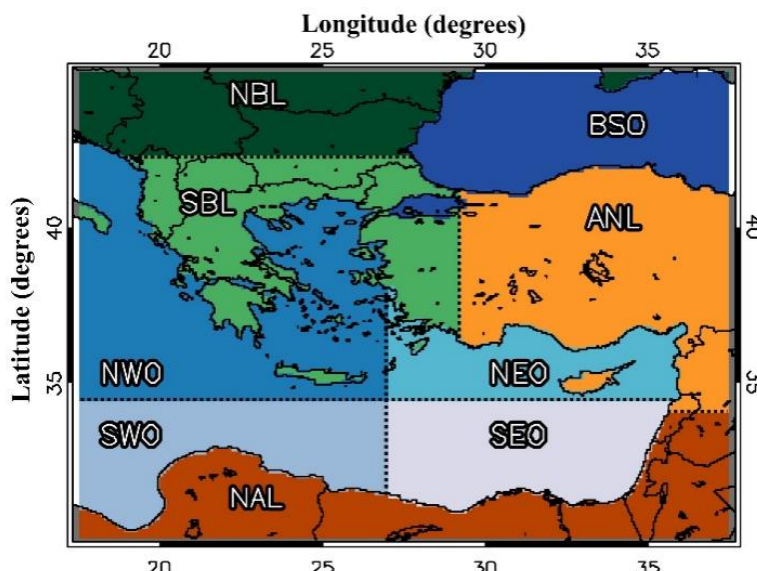


Figure 1. Eastern Mediterranean area map with the nine subregions of interest (NBL: Northern Balkans Land, SBL: Southern Balkans, ANL: Anatolia Land, NAL: Northern Africa Land, BSO: Black Sea Oceanic, NWO: Northwestern Oceanic, SWO: Southwestern Oceanic, NEO: Northeastern Oceanic and SEO: Southeastern Oceanic).

To investigate the annual and seasonal aerosol-cloud relationships over the Eastern Mediterranean and over the nine subregions that constitute it, we utilised a decade (July 2002–December 2012) of $0.1^\circ \times 0.1^\circ$ MODIS-based aerosol, cloud and water vapor parameters from the QUantifying the Aerosol Direct and Indirect Effect over Eastern Mediterranean (QUADIEEMS) high resolution dataset^[35]. Specifically, within QUADIEEMS AOD and Fine Mode Ratio (FMR) data from the MODIS Collection 5.1 level-2 (MYD04_L2) were gridded on a $0.1^\circ \times 0.1^\circ$ spatial resolution following a procedure described in detail in Georgoulias et al.^[14]. The MODIS data were then combined with ultraviolet (UV) Aerosol Index (AI) data from Earth Probe Total Ozone Mapping (TOMS)^[36] and Ozone Monitoring Instrument (OMI)^[37] space-borne sensors. In addition, data from the ERA-Interim and the Monitoring Atmospheric Composition and Climate (MACC) reanalysis projects^[38–40] and data from the Goddard Chemistry Aerosol Radiation and Transport (GOCART) chemistry-aerosol-transport model^[41], were used in conjunction with the MODIS data to calculate the contribution of different aerosol types to the total AOD. Note that MODIS FMR data were used only over the sea, since FMR data over land is not reliable^[2]. For this reason, data from MACC reanalysis projects were used instead, for the discrimination of different aerosol types over land^[14].

In this work, the total AOD, the anthropogenic AOD (AOD_{anthr}) and dust AOD (AOD_{dust}) from the MODIS/Aqua-based QUADIEEMS dataset were utilised (see Georgoulias et al.^[14] for details). To produce the QUADIEEMS gridded cloud and water vapor dataset, the MODIS level-2 data (Collection 5.1) were averaged on a daily basis for each $0.1^\circ \times 0.1^\circ$ grid cell weighting by the size of the overlapping surfaces defined by the MODIS pixels and the grid cell area. Note that we only used MODIS collection 5.1 data, since QUADIEEMS dataset has not been updated yet to Collection 6. However, as far as aerosols are concerned, it has to be stressed that the validity of the results is still high, since the trends between the two collections have not changed significantly^[13].

In addition, quasi-coincident data of Water Vapor at clear sky (WV), Cloud Cover (CC), Cloud Optical Depth (COD) and Cloud Top Pressure (CTP) were used, in conjunction with AOD (total/anthropogenic/dust), to study the

aerosol-cloud relationships at different altitudes following previous studies^[2,24]. According to Gryspeerdt et al.^[42], quasi-coincident aerosol-cloud data (provided in the same grid cell) ensure that data are close enough to each others and represent the total time-integrated effect of aerosol on clouds. The number of observations (NOO) of AOD, AOD_{anthr} and AOD_{dust} that was utilised for the calculation of the mean CC, COD and CTP over every region and for every season is illustrated in **Figure S1 (Supplementary Material)**.

To study the annual relationships of AOD-WV-CC, we separated the data into 0.1 AOD and 1 cm WV bins and calculated the mean CC value for each bin. The same methodology was followed for the investigation of AOD-WV-COD and AOD-WV-CTP relationships. By sorting the data into bins, we minimize the effect of spatial heterogeneity of local meteorology on AOD-WV-CC-COD-CTP co-variation^[43]. To avoid artifacts due to undersampling in our investigation, we only considered CC, COD and CTP values that had more than 30 values in each AOD-WV bin. In addition, we used CTP as a measure of cloud altitude, with high CTP values denoting clouds at low altitude and low CTP values denoting clouds at high altitude. Specifically, clouds with CTP > 800 hPa were considered as low boundary layer clouds, clouds with CTP between 400–800 hPa as medium height clouds and clouds with CTP > 400 hPa as high clouds^[24].

For the study of seasonal AOD-WV-CC, AOD-WV-COD and AOD-WV-CTP relationships we separated the whole data into four seasons. For winter, we used data of December, January and February (DJF), for spring, data of March, April and May (MAM), for summer, data of June, July and August (JJA) and for autumn, data of September, October and November (SON).

3. Results and Discussion

3.1. Aerosol-Cloud Relationships over the Eastern Mediterranean Region and Sub-Regions

Here, we present the results for total aerosols, anthropogenic aerosols and dust. We consider total aerosols as the sum of anthropogenic, dust, fine-mode natural (over land only) and marine (over the sea only) aerosols.

3.1.1. Total Aerosols-Cloud Relationships

The spatial distribution of quasi-coincident data of mean total AOD, CC, COD and WV, over the EMT region, is presented in **Figure 2**. Over NAL (along the northern coasts of Egypt, coasts of Lebanon and Israel), ANL (Turkey and along the coasts of Syria) and SBL regions (along the coasts of Greece) high values of AOD are observed (**Figure 2a**).

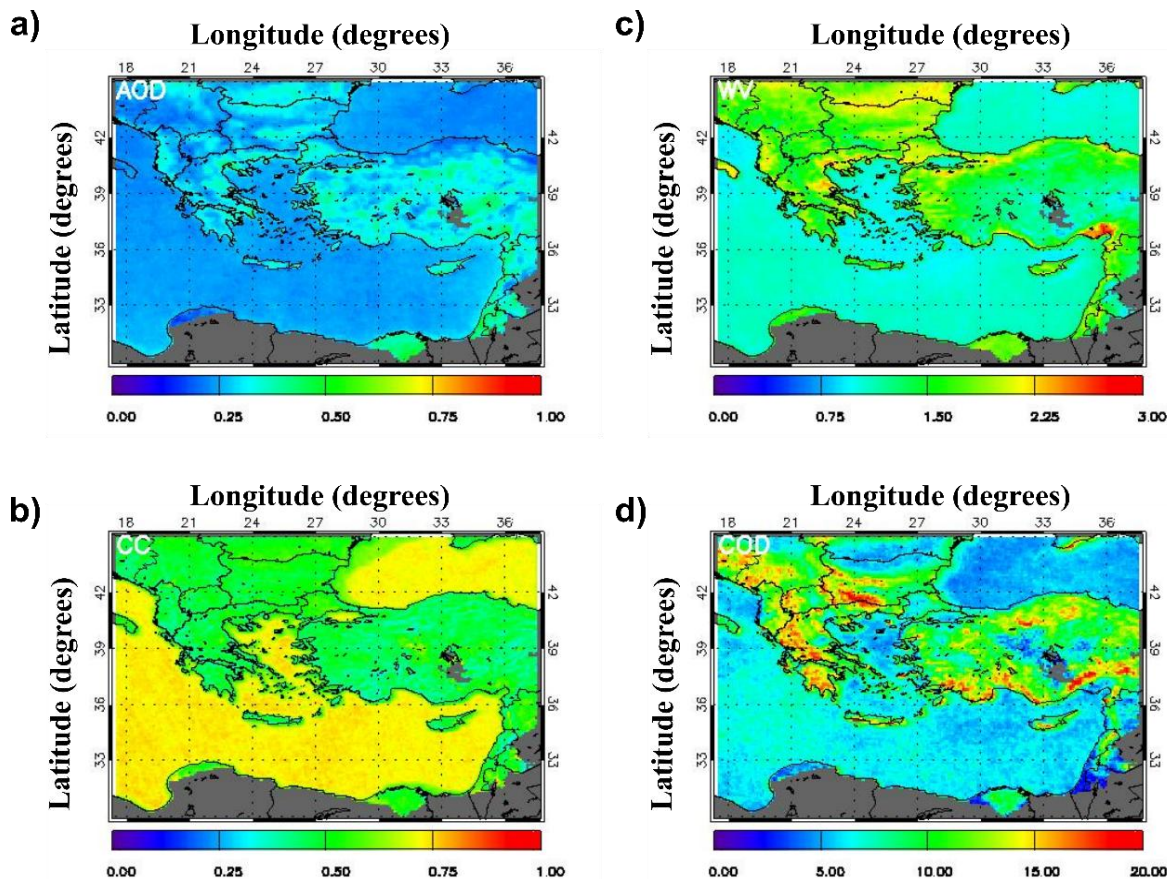
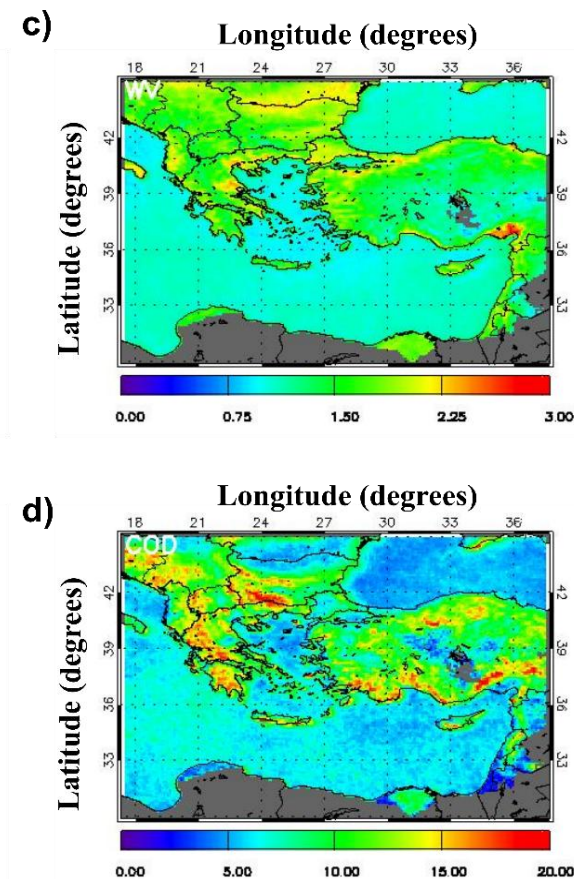


Figure 2. Spatial distribution of mean total Aerosol Optical Depth at 550 nm (AOD) (a), Cloud Cover (CC) (b), Water Vapor (WV) in cm (c) and Cloud Optical Depth (COD) (d), over the Eastern Mediterranean, for all seasons, for the period 2002–2012, from Aqua.

COD is found to have a different behavior according to WV amounts. For WVs between 5–6 cm, which are observed at CTP > 900 hPa, COD increases with increasing CC and aerosol loading, probably another sign of cloud invigoration by aerosols (**Figure 3**). For WVs between 3–4 cm, COD remains constant, while for WVs 1–2 cm, which are observed at CTP < 850 hPa, it decreases (**Figure 3b,e**). This decrease might be due to the radiative heating of absorbing aerosols inside or at the top of the clouds, which results in more WV evaporation and thinning of the clouds, an indication of the semi-direct effect^[13]. One the other hand, the

In addition, high values of CC are observed over all oceanic regions (NWO, SWO, SEO, NEO, BSO) (**Figure 2b**), while high WV concentrations are found over ANL (along south-eastern coasts of Turkey) and SBL regions (along northern coasts of Greece and Turkey) (**Figure 2c**). Finally, high values of COD are found over NBL, SBL and ANL regions (**Figure 2d**).



possibility that the reduction could be the result of the presence of dark aerosols above the clouds cannot be completely ruled out. Such aerosols have been observed to reduce cloud reflectance, which may result in a retrieval artifact observed by satellite^[44].

Figure 4 presents the aerosol-cloud relationships in summer, over all the Eastern Mediterranean Land regions (EML), namely NBL, SBL, ANL and NAL (**Figure 4a–c**), and over all the Eastern Mediterranean Oceanic regions (EMO), namely BSO, NWO, SWO, NEO and SEO (**Figure 4d–f**) as CC, COD and CTP difference ($\Delta CC = CC_{EMO} - CC_{EML}$)

CC_{EML} , $\Delta COD = COD_{EMO} - COD_{EML}$ and $\Delta CTP = CTP_{EMO} - CTP_{EML}$, respectively). ΔCC , ΔCOD and ΔCTP were calculated only for the common bins that had a CC, COD and CTP mean value from both EML and EMO regions. Our investigation shows that CC over the sea is larger than CC over land for most WV bins, a sign that aerosols affect clouds more significantly over the sea than over land (Figure 4a,d).

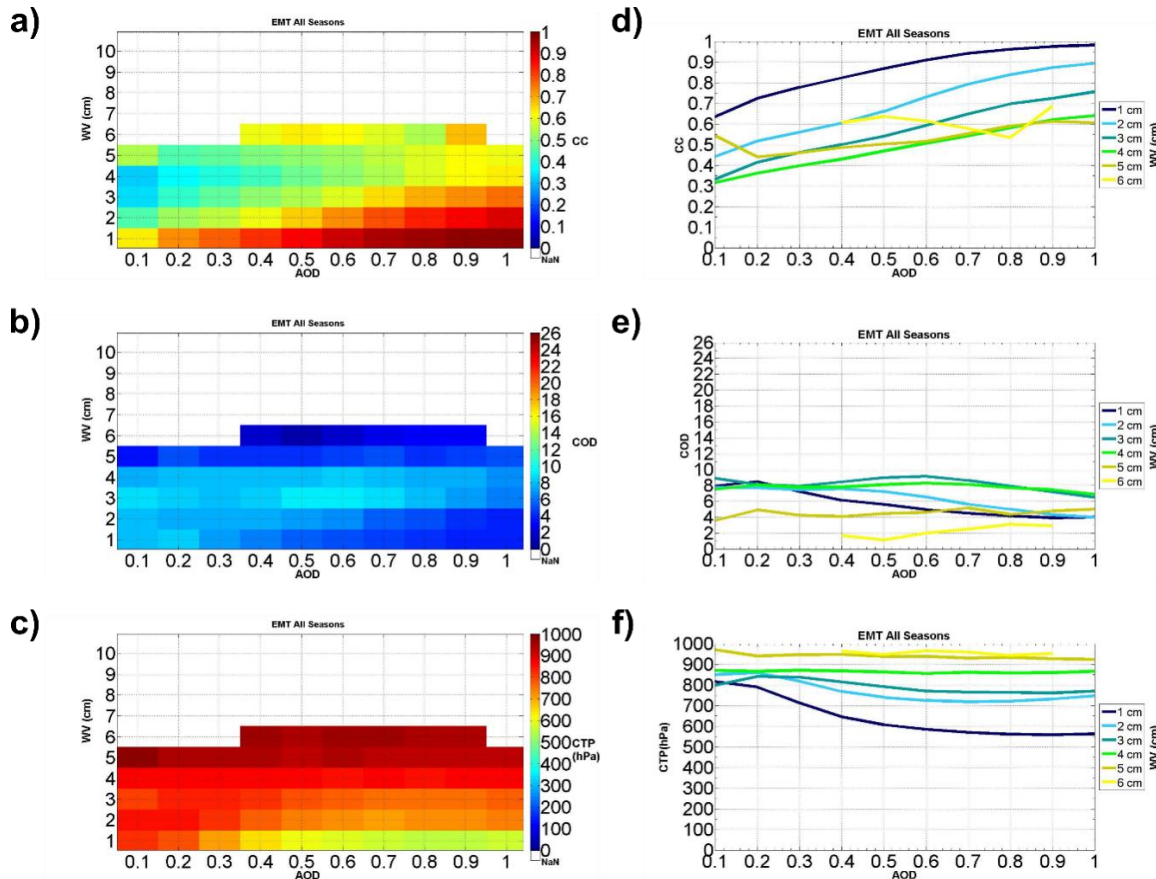


Figure 3. Mean total Aerosol Optical Depth at 550 nm (AOD)-Water Vapor (WV)-Cloud Cover (CC) relationships (a,d), mean total Aerosol Optical Depth at 550 nm (AOD)-Water Vapor (WV)-Cloud Optical Depth (COD) relationships (b,e) and mean total Aerosol Optical Depth at 550 nm (AOD)-Water Vapor (WV)-Cloud Top Pressure (CTP) relationships (c,f), over the Eastern Mediterranean for all seasons, from Aqua, for the period 2002–2012. Figures on the left present results in bins, while figures on the right present results as line graphs. The data were sorted into 0.1 AOD and 1 cm WV bins to minimize the effect of spatial heterogeneity of local meteorology. The color bars represent the average CC, COD and CTP values in each AOD and WV bin. NaN at the color bars denote less than 30 values in this bin.

COD over land is larger than COD over the sea, irrespective of WV and AOD amount (Figures 2d and 4b,e), in accordance with the findings of Peng et al. [46]. This might be another sign of greater aerosol invigoration effect over regions with strong convection [17,47,48], which is more pronounced over land than over the sea. In addition, according to Alexandri et al. [49], these COD maxima could be due to orographic clouds, over local geographical features, such

as mountain ranges. Over land, at low and moderately polluted conditions (AOD between 0.1–0.5), COD increases with increasing AOD, while at heavy polluted conditions (AOD between 0.6–1), it decreases or remains constant with increasing aerosol loading (Figure 4b,e). Over the sea, the same COD behavior is observed but for lower AOD bins. In particular, COD increases for AOD 0.1–0.2 and then decreases or remains constant (figure not shown). This may

indicate the existence of competition for water vapor, between the larger aerosol particles, which are more prone to water vapor condensation, and the smaller ones, resulting in a decrease in COD^[3,50,51]. Nonetheless, we cannot rule out that this decrease on COD may be due to a retrieval artifact, either from the insertion of carbonaceous aerosols within or above the cloud that darkens the cloud, or a sub-pixel dark surface contamination in the cloud reflectance measurement from the satellite^[45,46].

In spring and summer months and over all regions, CTP is found to decrease with increasing AOD (Figure 4c,f). Considering CTP as an indicator of the cloud-top height this may suggest an enhancement of cloud vertical structure^[1,52,53]. On the other hand, in autumn and winter

months and for high WV bins, CTP exhibits a reverse behavior with increasing aerosol loading, especially over land (Supplementary Material Figure S2c,f). According to Alam et al.^[54] and Tripathi et al.^[55], this might be due to the fact that the reduced updraft, that is usually observed in autumn and winter, do not favor the vertical transport of aerosol at higher altitude, while the strong updraft in spring and summer, facilitates the aerosol effect on clouds. For constant AOD and WV, clouds over land are found to be higher (lower CTP) than clouds over the nearby sea (higher CTP) regions (Figure 4c,f). According to Saponaro et al.^[56], this might be due to surface heating, resulting in stronger turbulence over land than over the sea, causing the clouds to rise higher.

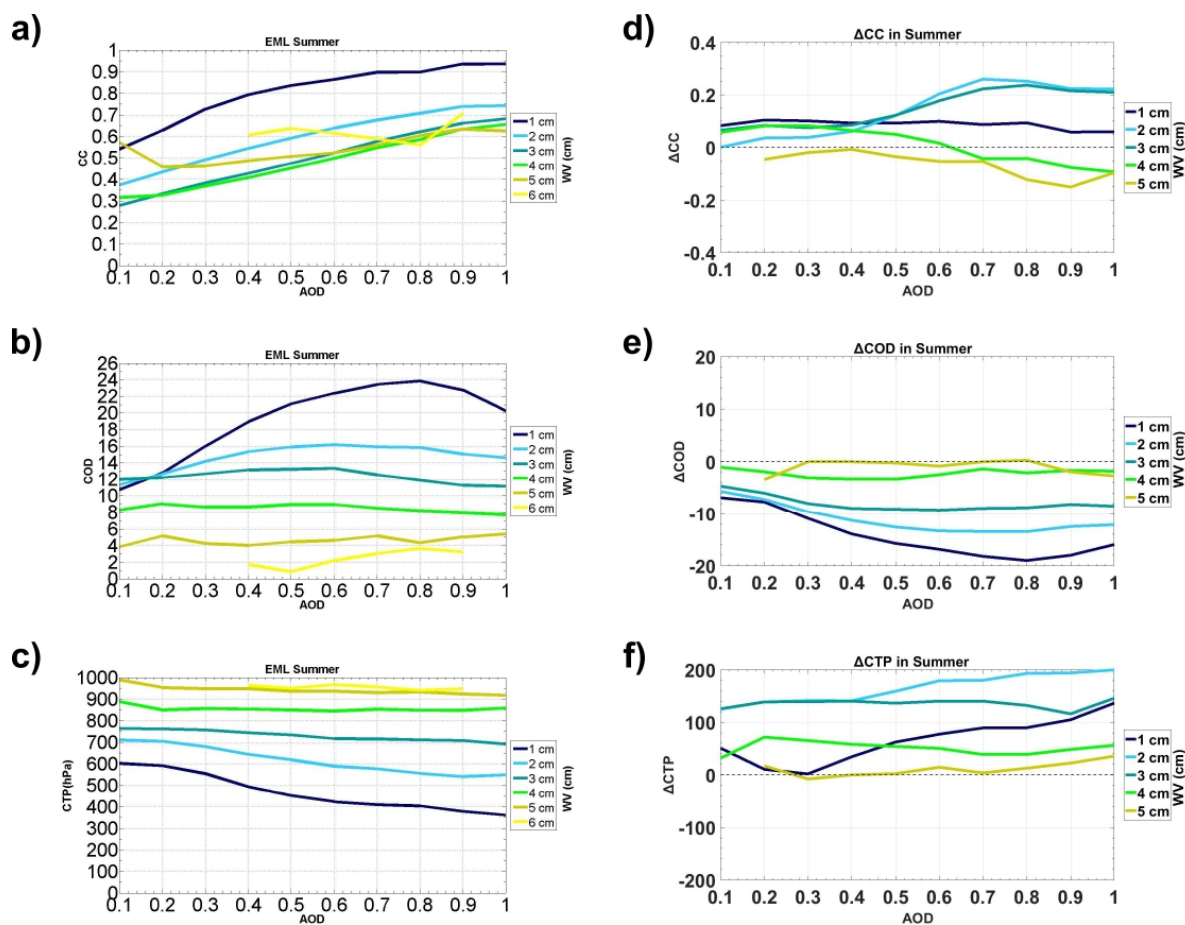


Figure 4. Mean total Aerosol Optical Depth at 550 nm (AOD)-Water Vapor (WV)-Cloud Cover (CC) relationships (a), mean total Aerosol Optical Depth at 550 nm (AOD)-Water Vapor (WV)-Cloud Optical Depth (COD) relationships (b) and mean total Aerosol Optical Depth at 550 nm (AOD)-Water Vapor (WV)-Cloud Top Pressure (CTP) relationships (c), over the Eastern Mediterranean Land region in summer, from Aqua, for the period 2002–2012. $\Delta CC = CC_{EMO} - CC_{EML}$ (d), $\Delta COD = COD_{EMO} - COD_{EML}$ (e), $\Delta CTP = CTP_{EMO} - CTP_{EML}$ (f), in summer.

3.1.2. Anthropogenic Aerosols-Cloud Relationships

For the investigation of anthropogenic aerosols-cloud relationships, we considered only anthropogenic AOD values (AOD_{anthr}) that were at least two times greater than dust AOD (AOD_{dust}) and marine-natural AOD ($AOD_{sea-nat}$), to avoid misleading inferences about the anthropogenic aerosols-cloud relationships, in case the amount of the other two types of aerosols was high enough to bias the results. Then, we followed the same method as above, separating the AOD_{anthr} , WV, CC, COD and CTP quasi-coincident data into 0.1 AOD_{anthr} and 1 cm WV bins and calculated the mean CC, COD and CTP values. As before, we only considered CC, COD and CTP values that had more than 30 values in

each AOD_{anthr} - WV bin.

The spatial distribution of quasi-coincident data of mean anthropogenic AOD, CC, COD and WV, over the EMT region, is presented in **Figure 5**. High values of AOD_{anthr} are found over NAL, NBL (eastern areas) and along the coasts of ANL and SBL regions (**Figure 5a**). CC is found to have high values over all oceanic regions EMO, NAL and ANL (central Turkey) regions (**Figure 5b**). In addition, high WV concentrations are observed over ANL (along the southern coasts of Turkey), SBL (along the northern coasts of Greece) and NBL (eastern areas) regions (**Figure 5c**), while high values of COD are found over NAL, ANL, SBL (along the coasts) and NBL (southern areas) regions (**Figure 5d**).

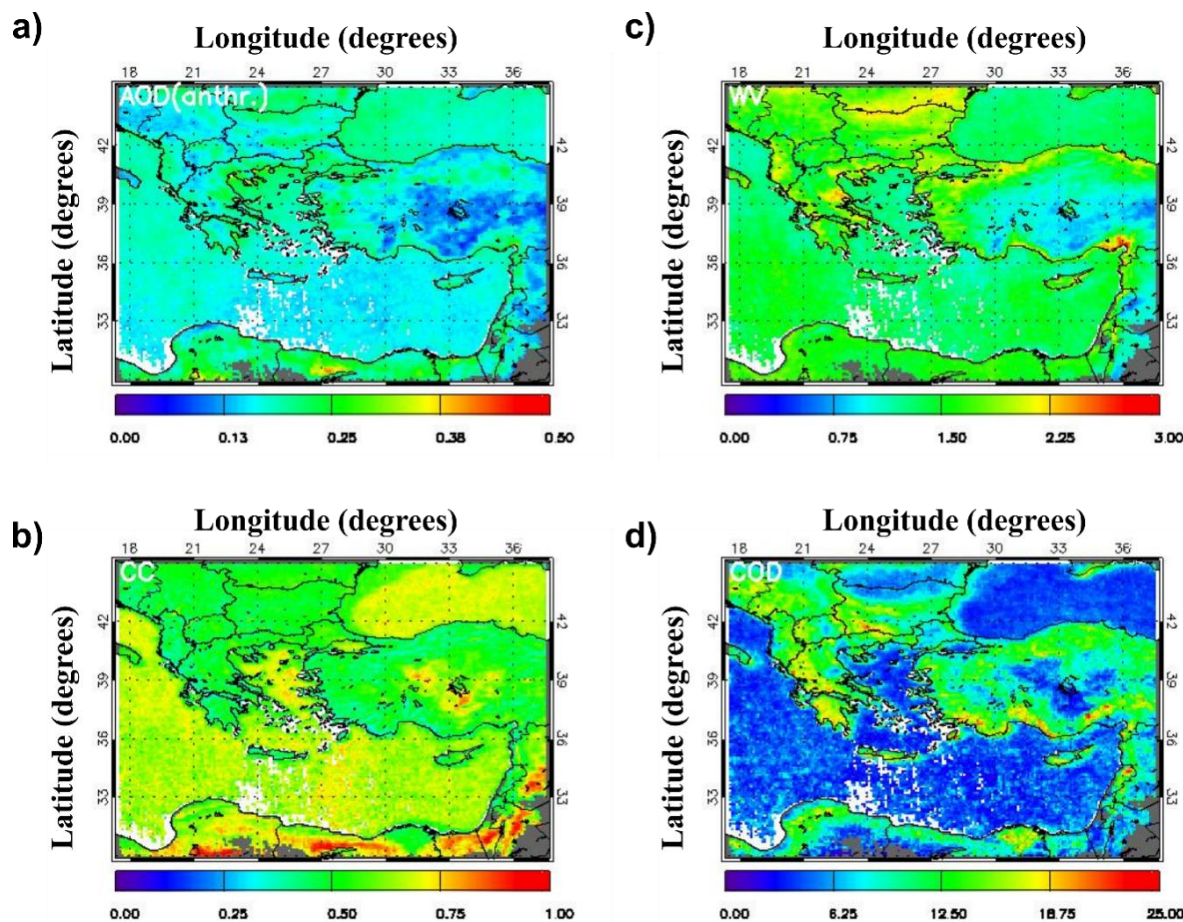


Figure 5. Spatial distribution of mean anthropogenic Aerosol Optical Depth at 550 nm ($AOD_{anthr.}$) (a), Cloud Cover (CC) (b), Water Vapor (WV) in cm (c) and Cloud Optical Depth (COD) (d), over the Eastern Mediterranean, for all seasons, for the period 2002–2012, from Aqua.

Over all regions, CC is found to increase with increasing anthropogenic aerosol loading, irrespective of WV bins

(**Figure 6a,d**), in accordance with previous studies^[2,24,57].

For WV between 5–6 cm, COD increases with increas-

ing aerosol loading. On the other hand, for WV between 1–4 cm, COD is found to increase with increasing AOD_{anthr} until AOD_{anthr} 0.4 and then to decrease (**Figure 6b,e**). This boomerang-shaped relationship between COD versus aerosol loading could be explained by a combination of physical processes and satellite retrieval artifacts. Aerosols within or above the clouds can absorb solar radiation, resulting in evaporating or thinning the cloud optically^[46,58]. At the same

time, these absorbing aerosols, by evaporating or thinning the cloud, can reveal a dark surface beneath it, reducing the visible reflectance received by the satellite, which is interpreted by the retrieval as a lower COD^[59]. As previously reported for total aerosol-cloud relationships, CC at high altitudes (low CTP) is higher than CC at low altitudes (high CTP), possibly due to the invigoration effect of anthropogenic aerosols on clouds (**Figure 6c,f**).

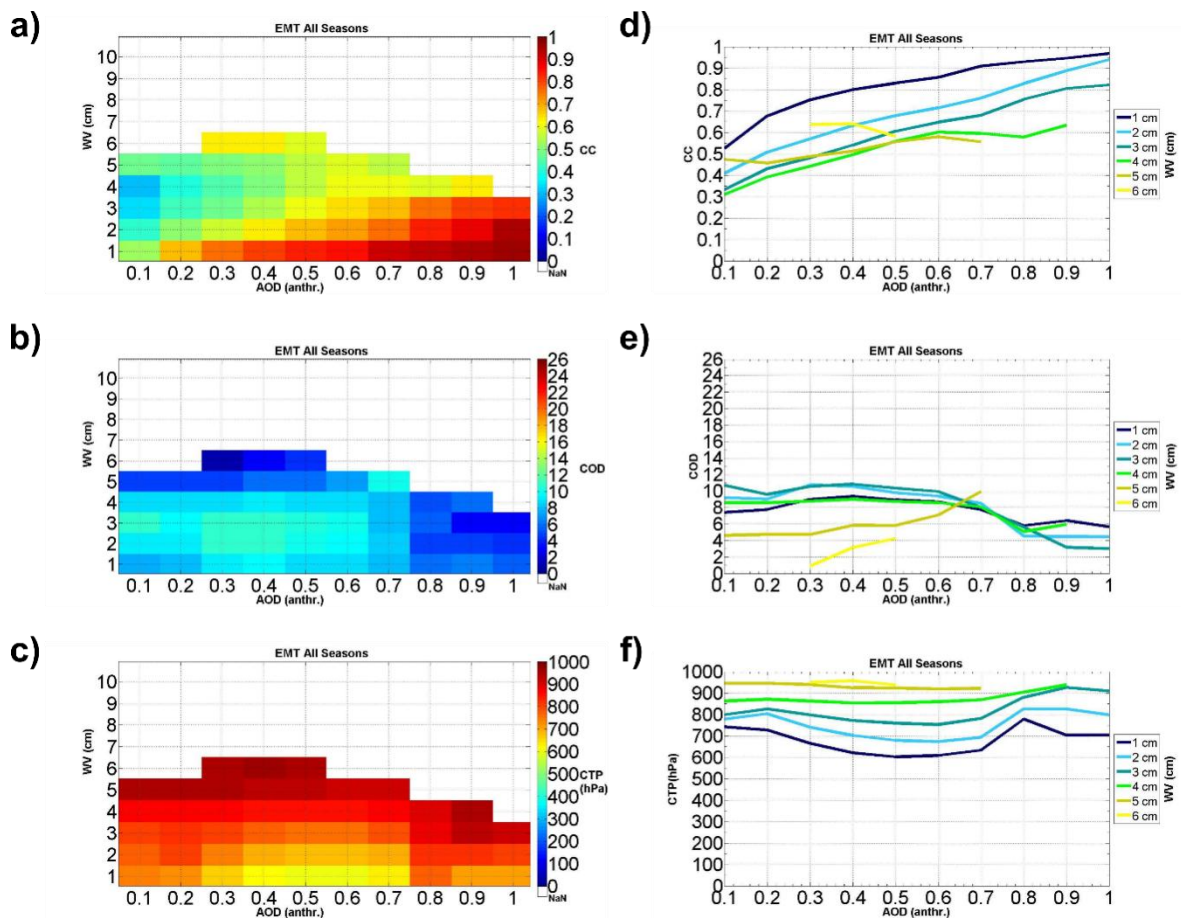


Figure 6. Mean anthropogenic Aerosol Optical Depth at 550 nm (AOD_{anthr})-Water Vapor (WV)-Cloud Cover (CC) relationships (a,d), mean anthropogenic Aerosol Optical Depth at 550 nm (AOD_{anthr})-Water Vapor (WV)-Cloud Optical Depth (COD) relationships (b,e) and mean anthropogenic Aerosol Optical Depth at 550 nm (AOD_{anthr})-Water Vapor (WV)-Cloud Top Pressure (CTP) relationships (c,f), over the Eastern Mediterranean for all seasons, from Aqua, for the period 2002–2012. Figures on the left present results in bins, while figures on the right present results as line graphs. The data were sorted into 0.1 (AOD_{anthr}) and 1 cm WV bins to minimize the effect of spatial heterogeneity of local meteorology. The color bars represent the average CC, COD and CTP values in each (AOD_{anthr}) and WV bin. NaN at the color bars denote less than 30 values in this bin.

In summer and for AOD_{anthr} between 0.1–0.4, CC over the sea is greater than CC over land, while for AOD_{anthr} higher than 0.5, the relationship is reversed (**Figure 7a,d**). This could be an indication, that the invigoration effect over land is stronger than over the sea, especially over regions

with $AOD > 0.5$.

Over land, where vast amounts of anthropogenic aerosols are emitted into the atmosphere and for WV between 5–6 cm, COD is found to increase with increasing AOD_{anthr} . On the other hand, for WV between 1–4 cm and

for $CTP < 900$ hPa, COD is found to increase until AOD_{anthr} 0.4 and then to decrease (**Figure 7b**). This reduction of COD could be attributed to the radiative effect of anthropogenic aerosols, resulting in thinning the clouds^[60]. However, we cannot rule out that this finding may be a retrieval artifact as well. For all WV and AOD_{anthr} bins, COD over land is larger than COD over ocean, probably due to the greater invigorating effect of anthropogenic aerosols on clouds over

land than over the sea^[52] (**Figures 5d** and **7e**).

For all WV and AOD_{anthr} bins, CTP over land is found to decrease with increasing AOD_{anthr} (**Figure 7c**). In addition, CTP over the sea, is higher than CTP over land, irrespective of WV and AOD_{anthr} bin, which implies that clouds over land are higher than clouds over the sea, probably due to greater surface heating, resulting in the formation of higher clouds^[56] (**Figure 7f**).

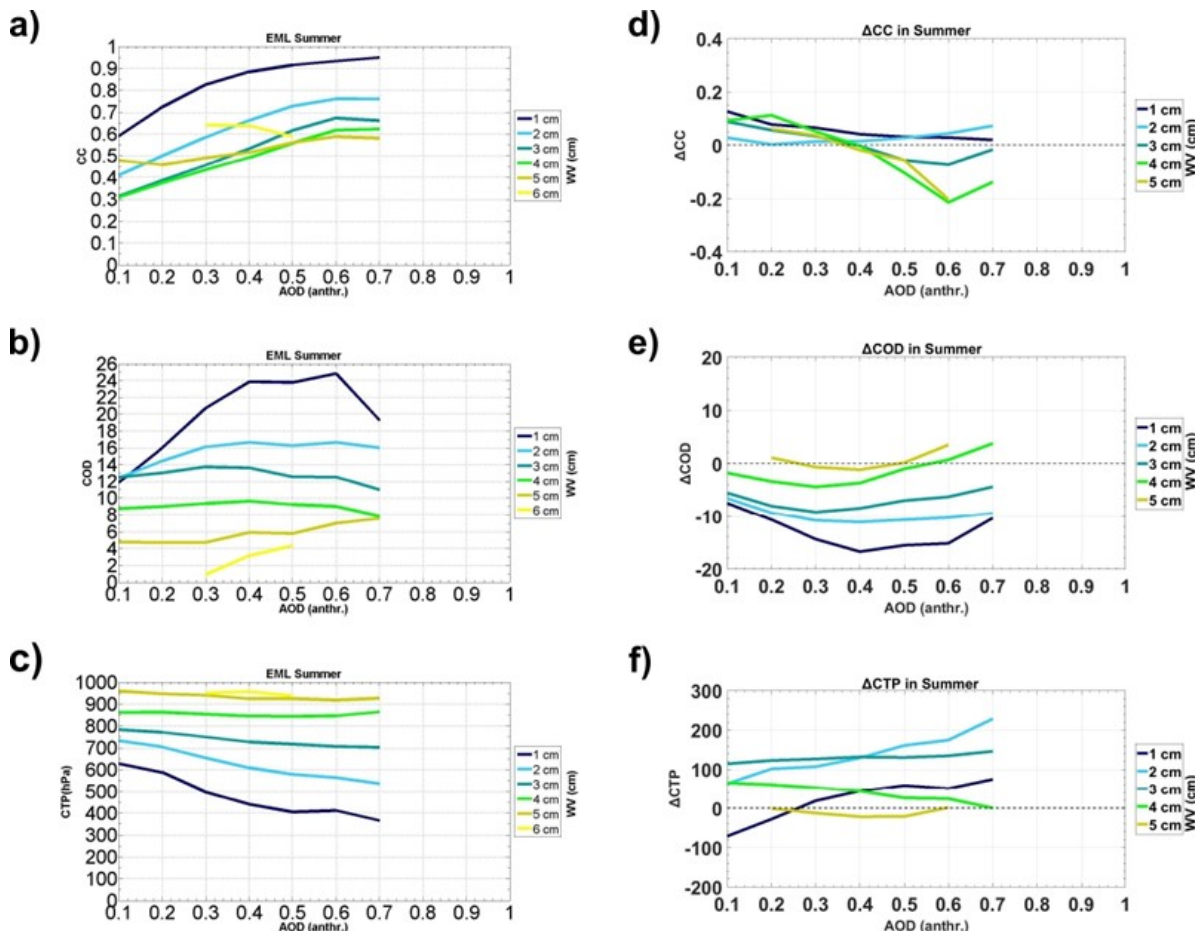


Figure 7. Mean anthropogenic Aerosol Optical Depth at 550 nm (AOD_{anthr})-Water Vapor (WV)-Cloud Cover (CC) relationships (a), mean anthropogenic Aerosol Optical Depth at 550 nm (AOD_{anthr})-Water Vapor (WV)-Cloud Optical Depth (COD) relationships (b) and mean anthropogenic Aerosol Optical Depth at 550 nm (AOD_{anthr})-Water Vapor (WV)-Cloud Top Pressure (CTP) relationships (c), over the Eastern Mediterranean Land regions in summer, from Aqua, for the period 2002–2012. $\Delta CC = CC_{EMO} - CC_{EML}$ (d), $\Delta COD = COD_{EMO} - COD_{EML}$ (e), $\Delta CTP = CTP_{EMO} - CTP_{EML}$ (f), in summer.

3.1.3. Dust-Cloud Relationships

For the study of dust-cloud relationships, we considered only dust AOD values (AOD_{dust}) that were at least two times greater than anthropogenic AOD (AOD_{anthr}) and marine-natural AOD ($AOD_{sea-nat}$). Then, we followed the previous methodology, separating the AOD_{dust} , WV, CC, COD and

CTP quasi-coincident data into 0.1 AOD_{dust} and 1 cm WV bins, and calculated the mean CC, COD and CTP values. As before, we only considered CC, COD and CTP values that had more than 30 values in each AOD_{dust} -WV bin.

High values of AOD_{dust} are found over NAL region (**Figure 8a**), while increased CC is observed over SWO, SEO, NEO and NWO regions (**Figure 8b**). In addition, high

concentrations of WV are found over NAL and along the coasts of ANL and SBL regions (**Figure 8c**). Finally, high

values of COD are observed along the coasts of SBL and ANL regions (**Figure 8d**).

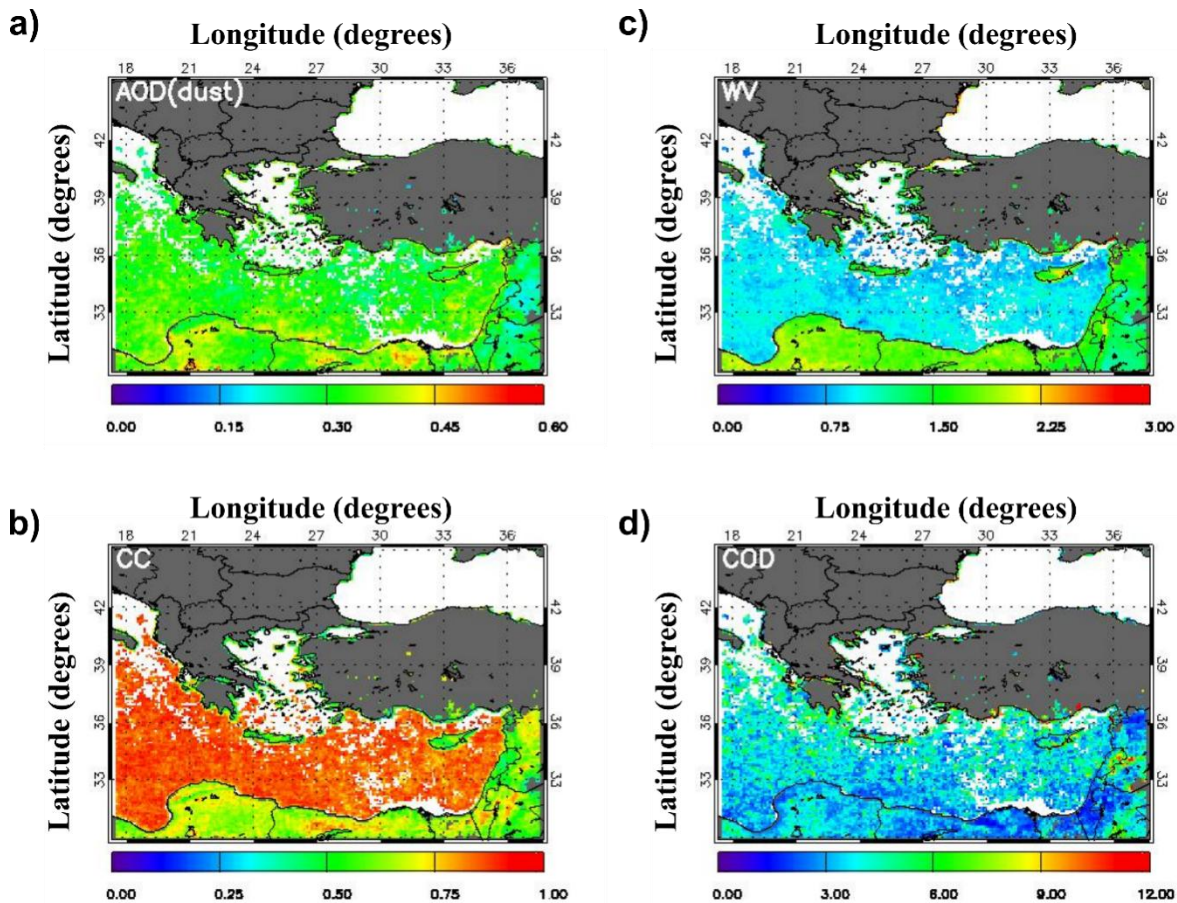


Figure 8. Spatial distribution of mean dust Aerosol Optical Depth at 550 nm (AOD_{dust}) (a), Cloud Cover (CC) (b), Water Vapor (WV) (c) and Cloud Optical Depth (COD) (d), over the Eastern Mediterranean, for all seasons, for the period 2002–2012, from Aqua.

Over all regions and irrespective of season and WV bin, CC is found to increase with increasing AOD_{dust} (**Figure 9a,d**). Over all regions and for all seasons, dust COD is observed to have values less than 8, irrespective of WV and AOD_{dust} bins (**Figure 9b,e**). In addition, it is evident that anthropogenic COD is larger than dust COD, which in some cases (specific WV and AOD_{dust} bins) might be of about 82% (**Figures 6e** and **9e**) (see **Figures 5d** and **8d** as well). According to Harikishan et al.^[17], this reduction of cloud depth could be due to the fact that dust above the clouds may absorb incoming solar radiation, increasing the ambient temperature through the adiabatic warming of dust. This, in turn, leads to a decay of relative humidity available for cloud growth, inhibiting cloud formation. In addition, anthropogenic aerosols tend to be smaller and

more hygroscopic than dust, allowing them to act more effectively as cloud condensation nuclei. This can increase the cloud droplet number concentration, resulting in higher COD^[61–63].

In most cases, CTP is found to decrease as AOD_{dust} increases (**Figure 9c,f**), suggesting an enhancement of cloud vertical structure^[1].

Finally, our investigation shows that, for AOD_{dust} > 0.3 and for WV between 3–4 cm, even though CC over land is higher than CC over the sea (**Figure 10a,d**), the respective COD and CTP over land are lower than COD (**Figure 10b,e**) and CTP over the sea (**Figure 10c,f**). On the other hand, for WV between 1–2 cm, CC over land is lower than CC over the sea (**Figure 10a,d**), while the respective COD and CTP over land are higher than COD (**Figure 10b,e**) and CTP over

the sea (Figure 10c,f). This could be another sign of the greater invigorating effect of dust on clouds over land than over the sea.

A general summary of the seasonal trends of aerosol - cloud relationships over the region can be found in the **Supplementary Material (Table S1)**.

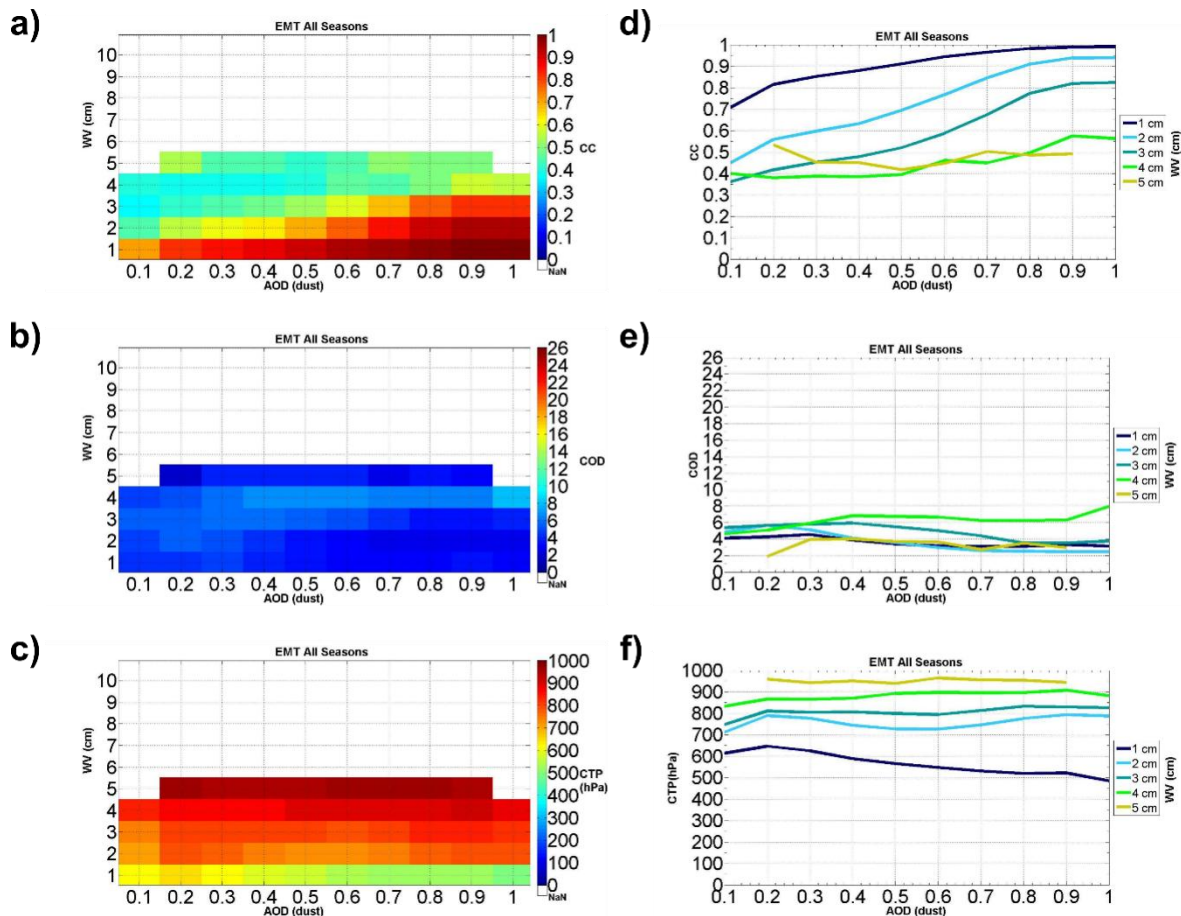


Figure 9. Mean dust Aerosol Optical Depth at 550 nm (AOD_{dust})-Water Vapor (WV)-Cloud Cover (CC) relationships (a,d), mean dust Aerosol Optical Depth at 550 nm (AOD_{dust})-Water Vapor (WV)-Cloud Optical Depth (COD) relationships (b,e) and mean dust Aerosol Optical Depth at 550 nm (AOD_{dust})-Water Vapor (WV)-Cloud Top Pressure (CTP) relationships (c,f), over the Eastern Mediterranean for all seasons, from Aqua, for the period 2002–2012. Figures on the left present results in bins, while figures on the right present results as line graphs. The data were sorted into 0.1 (AOD_{dust}) and 1 cm WV bins to minimize the effect of spatial heterogeneity of local meteorology. The color bars represent the average CC, COD and CTP values in each (AOD_{dust}) and WV bin. NaN at the color bars denote less than 30 values in this bin.

3.2. Limitations and Uncertainties

The challenge in all aerosol-cloud interaction studies that utilise remote sensing and model data is to minimise the uncertainties of the results. These uncertainties may be attributable to the complicated relations between aerosols and clouds in the atmosphere under different water vapor environments and altitudes, as well as due to seasonal, geographical and instrumental variations. In the present study,

in order to minimize the effect of seasonality, the data was separated into four seasons. In addition, the selection of each region was chosen to ensure the inclusion of a statistically significant number of observations, while maintaining the condition of relative homogeneity in terms of dynamic and thermodynamic parameters. Furthermore, in order to minimize the effect of spatial heterogeneity of local meteorology on AOD-WV-CC-COD-CTP co-variation, our data was separated into different bins^[43].

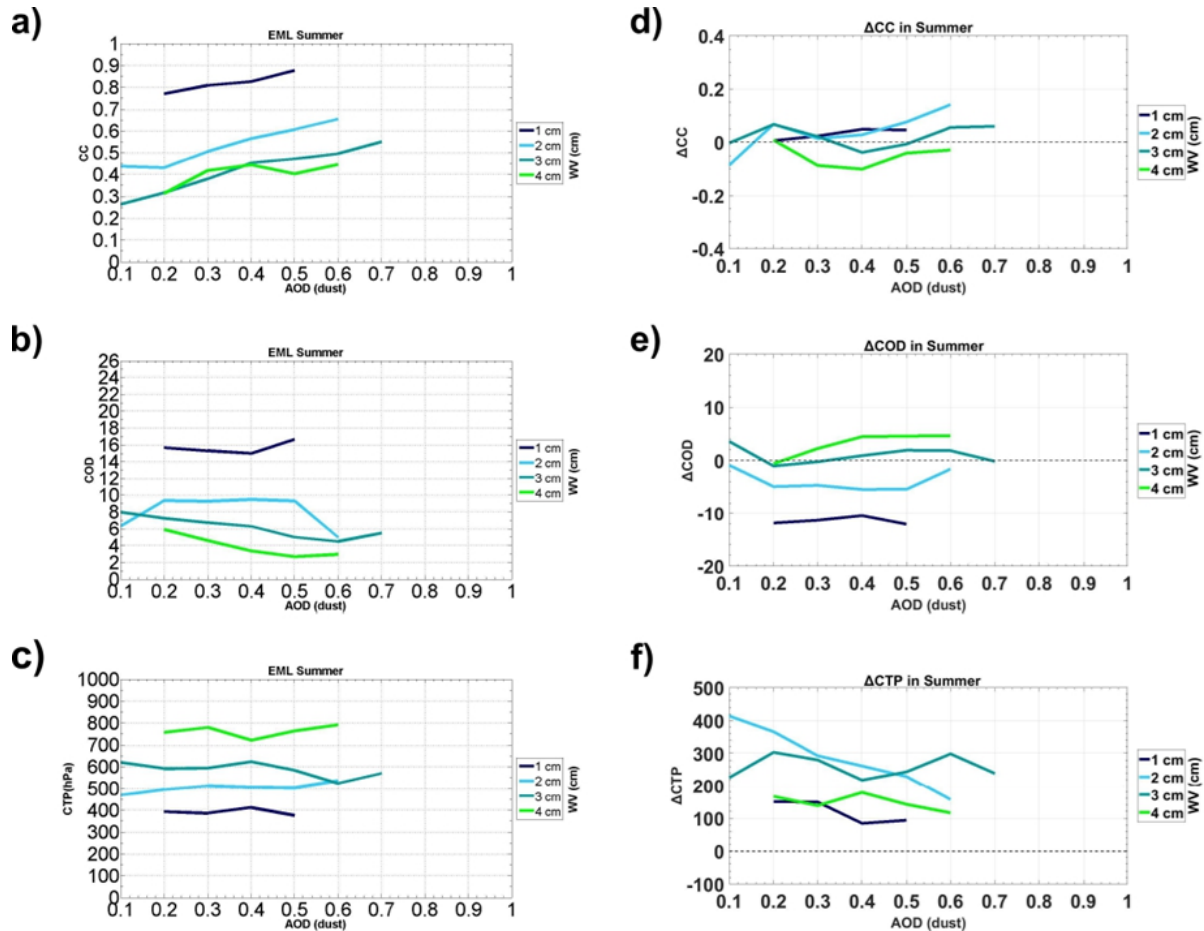


Figure 10. Mean dust Aerosol Optical Depth at 550 nm (AOD_{dust})-Water Vapor (WV)-Cloud Cover (CC) relationships (a), mean dust Aerosol Optical Depth at 550 nm (AOD_{dust})-Water Vapor (WV)-Cloud Optical Depth (COD) relationships (b) and mean dust Aerosol Optical Depth at 550 nm (AOD_{dust})-Water Vapor (WV)-Cloud Top Pressure (CTP) relationships (c), over the Eastern Mediterranean Land regions in summer, from Aqua, for the period 2002–2012. $\Delta CC = CC_{EMO} - CC_{EML}$ (d), $\Delta COD = COD_{EMO} - COD_{EML}$ (e), $\Delta CTP = CTP_{EMO} - CTP_{EML}$ (f), in summer.

However, a number of uncertainties still remain, arising from a combination of instrumental limitations, atmospheric complexity and methodological assumptions. The quality of remote sensing data is dependent on the calibration of the sensor, the spatial resolution, and the efficacy of cloud masking algorithms. In our study, we used MODIS aerosol and cloud products at a spatial resolution of appr. 10 km, which in complex terrains or near coastlines can smooth the real variation between them^[29]. The uncertainty of the MODIS AOD has been calculated to be approximately $\pm(0.05 + 0.15 AOD)$ over land and $\pm(0.03 + 0.05 AOD)$ over ocean^[28,64]. The uncertainties of the calculated AOD_{anthr} and AOD_{dust} are similar to the ones presented in Bellouin et al.^[65]. Specifically, AOD_{anthr} can be specified with an uncertainty of approximately 23% over land and 16% over the oceanic regions,

while AOD_{dust} can be specified with an uncertainty of approximately 19% over land and 33% over the oceanic regions. In addition, the presence of dark aerosols above the clouds have been observed to reduce cloud reflectance, which may result in a retrieval artifact observed by the MODIS instrument^[54]. Furthermore, observations from the MODIS instrument provide column-integrated data, thereby hindering the precise calculation of the vertical profiles of humidity and aerosol distribution.

Additionally, in the present study, AOD was utilised as a proxy for aerosol loading, which does not directly account for aerosol hygroscopicity. Future research integrating in situ observations, vertical profile data and modelling approaches may help address these limitations and improve our understanding of aerosol–cloud interactions.

4. Conclusions

In this work, we used a decade (July 2002–December 2012) of MODIS/Aqua-based aerosol, cloud and water vapor data from the QUantifying the Aerosol Direct and Indirect Effect over Eastern Mediterranean (QUADIEEMS) $0.1^\circ \times 0.1^\circ$ high resolution dataset^[14] for the Eastern Mediterranean Territory (EMT) and for nine urban and rural land and oceanic subregions.

Over all regions and seasons and WV bins, CC is found to increase with increasing total AOD. This increase might be of the order of 55% in summer for AOD 0.1–0.5, pointing towards the aerosol invigoration effect on clouds. In addition, COD is found to have a varied behavior depending on WV. For high WV values (5–6 cm), COD increases with CC and aerosol loading, which is another indication of aerosol invigoration effect on clouds. On the other hand, for low WV values (1–2 cm) COD decreases with increasing CC and AOD, probably due to the semi-direct effect or to a retrieval artifact. Furthermore, CTP is found to decrease with increasing AOD in spring and summer, but in autumn and winter this behavior is reversed (CTP increases), especially over land and for high WV environments. This may be due to the differences in updraft speed among the seasons.

Regarding the relationships between AOD_{anthr} and clouds, CC is observed to increase with AOD_{anthr} for all WV bins, regions and seasons. Additionally, COD presents a “boomerang-shaped” response; for WV 1–4 cm COD increases at low and moderately polluted conditions ($AOD_{anthr} < 0.5$) and then decreases or remains constant. This could be attributed to the existence of competition for water vapor between the larger aerosol particles and the smaller ones at heavy pollution conditions, without ruling out the possibility that this behavior could be a satellite retrieval artifact, or a sign of the semi-direct effect. Moreover, CTP is found to decrease with increasing AOD_{anthr} over land, probably due to the aerosol invigoration effect on clouds.

Concerning the relationships between AOD_{dust} and clouds, CC is found to increase with AOD_{dust} irrespective of WV bins, regions and seasons, underscoring the active role of mineral dust in cloud droplet activation and cloud formation. Furthermore, dust COD is observed to be lower than anthropogenic COD, which in some cases (specific WV and AOD bins) might be about 82%. This reduced COD

may be the result of dust’s ability to absorb solar radiation above clouds, warming the layer and suppressing further condensation and cloud thickening. In addition, this could be due to anthropogenic aerosols being smaller and more hygroscopic than dust, which increases the cloud droplet number concentration, resulting in higher COD. As before, CTP is found to decrease with increasing AOD_{dust} , pointing again to the aerosol invigoration effect on clouds, especially for WV bins 3–4 cm and $AOD_{dust} > 0.3$.

From our study, some differences between land and oceanic regions were also observed. Specifically, CC is found typically higher over oceans than land, except at very high WV (5 cm), likely due to the urban or orographic influences over land. Moreover, COD is consistently higher over land, regardless of AOD and WV, reflecting stronger convection and the influence of orographic clouds.

Supplementary Materials

The following supporting information can be downloaded at https://journals.bilpubgroup.com/files/Stathopoulou-S.etal.,2025_sup.pdf.

Author Contributions

Conceptualization, S.S., K.K. and A.G.; methodology, S.S., K.K. and A.G.; software, S.S.; validation, S.S., K.K. and A.G.; formal analysis, S.S., K.K. and A.G.; investigation, S.S., K.K. and A.G.; resources, S.S.; data curation, S.S., and A.G.; writing—original draft preparation, S.S.; writing—review and editing, S.S., K.K. and A.G.; visualization, S.S., A.G.; supervision, K.K. and A.G.; project administration, K.K.; funding acquisition, K.K. All authors have read and agreed to the published version of the manuscript.

Funding

This research has been partially financed under the FP7 Programme MarcoPolo (Grant Number 606953, Theme SPA.2013.3.2-01), and the corresponding Matching Funds.

Institutional Review Board Statement

Not applicable.

Informed Consent Statement

Not applicable.

Data Availability Statement

Data is available upon request.

Acknowledgments

The authors would like to thank Aristeidis Georgoulas for the provision of the QUADIEEMS dataset and his valuable insights during the research. The authors would also like to thank NASA Goddard Space Flight Center (GSFC) Level 1 and Atmosphere Archive and Distribution System (LAADS) (<http://ladsweb.nascom.nasa.gov>) for providing MODIS/Aqua Collection 5.1 level-2 daily aerosol, cloud and water vapor data, ECMWF (www.ecmwf.int) for the provision of the ERA-Interim and MACC reanalysis data and NASA's GIOVANNI web database (<http://giovanni.gsfc.nasa.gov/giovanni/>) for the provision of Aerosol Index data from Earth Probe TOMS and OMI and aerosol data from the GOCART chemistry-aerosol-transport model which were used for the production of the QUADIEEMS dataset. The authors would also like to thank the anonymous reviewers for their detailed comments and suggestions that substantially improved the quality of this manuscript.

Conflicts of Interest

The authors declare no conflict of interest.

References

[1] Koren, I., Kaufman, Y.J., Rosenfeld, D., et al., 2005. Aerosol Invigoration and Restructuring of Atlantic Convective Clouds. *Geophysical Research Letters*. 32(14). DOI: <https://doi.org/10.1029/2005GL023187>

[2] Kourtidis, K., Stathopoulos, S., Georgoulas, A.K., et al., 2015. A Study of the Impact of Synoptic Weather Conditions and Water Vapor on Aerosol-Cloud Relationships over Major Urban Clusters of China. *Atmospheric Chemistry and Physics*. 15, 10955–10964. DOI: <https://doi.org/10.5194/acp-15-10955-2015>

[3] Liu, Y., de Leeuw, G., Kerminen, V.-M., et al., 2017. Analysis of Aerosol Effects on Warm Clouds over the Yangtze River Delta from Multi-Sensor Satellite Observations. *Atmospheric Chemistry and Physics*. 17, 5623–5641. DOI: <https://doi.org/10.5194/acp-17-5623-2017>

[4] Sena, E.T., McComiskey, A., Feingold, G., 2016. A Long-Term Study of Aerosol–Cloud Interactions and Their Radiative Effect at the Southern Great Plains Using Ground-Based Measurements. *Atmospheric Chemistry and Physics*. 16, 11301–11318. DOI: <https://doi.org/10.5194/acp-16-11301-2016>

[5] Twomey, S., 2007. Pollution and the Planetary Albedo. *Atmospheric Environment*. 41, 120–125. DOI: <https://doi.org/10.1016/j.atmosenv.2007.10.062>

[6] Albrecht, B.A., 1989. Aerosols, Cloud Microphysics, and Fractional Cloudiness. *Science*. 245, 1227–1230. DOI: <https://doi.org/10.1126/science.245.4923.1227>

[7] Ackerman, A.S., Toon, O.B., Stevens, D.E., et al., 2000. Reduction of Tropical Cloudiness by Soot. *Science*. 288, 1042–1047. DOI: <https://doi.org/10.1126/science.288.5468.1042>

[8] Johnson, B.T., Shine, K.P., Forster, P.M., 2004. The Semi-Direct Aerosol Effect: Impact of Absorbing Aerosols on Marine Stratocumulus. *Quarterly Journal of the Royal Meteorological Society*. 130, 1407–1422. DOI: <https://doi.org/10.1256/qj.03.61>

[9] Koch, D., Del Genio, A.D., 2010. Black Carbon Semi-Direct Effects on Cloud Cover: Review and Synthesis. *Atmospheric Chemistry and Physics*. 10, 7685–7696. DOI: <https://doi.org/10.5194/acp-10-7685-2010>

[10] Hatzianastassiou, N., Gkikas, A., Mihalopoulos, N., et al., 2009. Natural versus Anthropogenic Aerosols in the Eastern Mediterranean Basin Derived from Multiyear TOMS and MODIS Satellite Data. *Journal of Geophysical Research: Atmospheres*. 114. DOI: <https://doi.org/10.1029/2009JD011982>

[11] Lelieveld, J., Berresheim, H., Borrmann, S., et al., 2002. Global Air Pollution Crossroads over the Mediterranean. *Science*. 298, 794–799. DOI: <https://doi.org/10.1126/science.1075457>

[12] Mihalopoulos, N., Stephanou, E., Kanakidou, M., et al., 1997. Tropospheric Aerosol Ionic Composition in the Eastern Mediterranean Region. *Tellus Series B*. 49, 314–326. DOI: <https://doi.org/10.1034/j.1600-0889.49.issue3.7.x>

[13] Georgoulas, A.K., Alexandri, G., Kourtidis, K.A., et al., 2016. Differences between the MODIS Collection 6 and 5.1 Aerosol Datasets over the Greater Mediterranean Region. *Atmospheric Environment*. 147, 310–319. DOI: <https://doi.org/10.1016/j.atmosenv.2016.10.014>

[14] Georgoulas, A.K., Alexandri, G., Kourtidis, K.A., et al., 2016. Spatiotemporal Variability and Contribution of Different Aerosol Types to the Aerosol Optical Depth over the Eastern Mediterranean. *Atmospheric Chemistry and Physics*. 16, 13853–13884. DOI: <https://doi.org/10.5194/acp-16-13853-2016>

[15] Kanakidou, M., Mihalopoulos, N., Kindap, T., et al.,

2011. Megacities as Hot Spots of Air Pollution in the East Mediterranean. *Atmospheric Environment*. 45, 1223–1235. DOI: <https://doi.org/10.1016/j.atmosenv.2010.11.048>

[16] Papadimas, C.D., Hatzianastassiou, N., Mihalopoulos, N., et al., 2008. Spatial and Temporal Variability in Aerosol Properties over the Mediterranean Basin Based on 6-Year (2000–2006) MODIS Data. *Journal of Geophysical Research*. 113, D11205. DOI: <https://doi.org/10.1029/2007JD009189>

[17] Harikishan, G., Padmakumari, B., Maheskumar, R.S., et al., 2015. Radiative Effect of Dust Aerosols on Cloud Microphysics and Meso-Scale Dynamics during Monsoon Breaks over Arabian Sea. *Atmospheric Environment*. 105, 22–31. DOI: <https://doi.org/10.1016/j.atmosenv.2015.01.037>

[18] Tutsak, E., Koçak, M., 2020. Optical and Microphysical Properties of the Columnar Aerosol Burden over the Eastern Mediterranean: Discrimination of Aerosol Types. *Atmospheric Environment*. 229, 117463. DOI: <https://doi.org/10.1016/j.atmosenv.2020.117463>

[19] Balis, D.S., Amiridis, V., Zerefos, C., et al., 2003. Raman Lidar and Sunphotometric Measurements of Aerosol Optical Properties over Thessaloniki, Greece during a Biomass Burning Episode. *Atmospheric Environment*. 37, 4529–4538. DOI: [https://doi.org/10.1016/S1352-2310\(03\)00581-8](https://doi.org/10.1016/S1352-2310(03)00581-8)

[20] Meloni, D., di Sarra, A., Pace, G., et al., 2006. Aerosol Optical Properties at Lampedusa (Central Mediterranean). 2. Determination of Single Scattering Albedo at Two Wavelengths for Different Aerosol Types. *Atmospheric Chemistry and Physics*. 6, 715–727. DOI: <https://doi.org/10.5194/acp-6-715-2006>

[21] Pace, G., di Sarra, A., Meloni, D., et al., 2006. Aerosol Optical Properties at Lampedusa (Central Mediterranean). 1. Influence of Transport and Identification of Different Aerosol Types. *Atmospheric Chemistry and Physics*. 6, 697–713. DOI: <https://doi.org/10.5194/acp-6-697-2006>

[22] Methymaki, G., Bossioli, E., Boucouvala, D., et al., 2023. Brown Carbon Absorption in the Mediterranean Basin from Local and Long-Range Transported Biomass Burning Air Masses. *Atmospheric Environment*. 306, 119822. DOI: <https://doi.org/10.1016/j.atmosenv.2023.119822>

[23] Kalivitis, N., Gerasopoulos, E., Vrekoussis, M., et al., 2007. Dust Transport over the Eastern Mediterranean Derived from Total Ozone Mapping Spectrometer, Aerosol Robotic Network, and Surface Measurements. *Journal of Geophysical Research: Atmospheres*. 112, 1–9. DOI: <https://doi.org/10.1029/2006JD007510>

[24] Stathopoulos, S., Georgoulias, A.K., Kourtidis, K., 2017. Space-Borne Observations of Aerosol - Cloud Relations for Cloud Systems of Different Heights. *Atmospheric Research*. 183, 191–201. DOI: <https://doi.org/10.1016/j.atmosres.2016.09.005>

[25] Amiridis, V., Giannakaki, E., Balis, D.S., et al., 2010. Smoke Injection Heights from Agricultural Burning in Eastern Europe as Seen by CALIPSO. *Atmospheric Chemistry and Physics*. 10, 11567–11576. DOI: <https://doi.org/10.5194/acp-10-11567-2010>

[26] Levy, R.C., Remer, L.A., Dubovik, O., 2007. Global Aerosol Optical Properties and Application to Moderate Resolution Imaging Spectroradiometer Aerosol Retrieval over Land. *Journal of Geophysical Research*. 112, D13210. DOI: <https://doi.org/10.1029/2006JD007815>

[27] Chu, D.A., Kaufman, Y.J., Ichoku, C., et al., 2002. Validation of MODIS Aerosol Optical Depth Retrieval over Land. *Geophysical Research Letters*. 29, 8007. DOI: <https://doi.org/10.1029/2001GL013205>

[28] Levy, R.C., Remer, L.A., Kleidman, R.G., et al., 2010. Global Evaluation of the Collection 5 MODIS Dark-Target Aerosol Products over Land. *Atmospheric Chemistry and Physics*. 10, 10399–10420. DOI: <https://doi.org/10.5194/acp-10-10399-2010>

[29] Remer, L.A., Kaufman, Y.J., Tanré, D., et al., 2005. The MODIS Aerosol Algorithm, Products, and Validation. *Journal of the Atmospheric Sciences*. 62, 947–973. DOI: <https://doi.org/10.1175/JAS3385.1>

[30] Hsu, N.C., Tsay, S.C., King, M.D., et al., 2004. Aerosol Properties over Bright-Reflecting Source Regions. *IEEE Transactions on Geoscience and Remote Sensing*. 42, 557–569. DOI: <https://doi.org/10.1109/TGRS.2004.824067>

[31] Tanré, D., Kaufman, Y.J., Herman, M., et al., 1997. Remote Sensing of Aerosol Properties over Oceans Using the MODIS/EOS Spectral Radiances. *Journal of Geophysical Research: Atmospheres*. 102, 16971–16988. DOI: <https://doi.org/10.1029/96jd03437>

[32] Ackerman, S.A., Strabala, K.I., Menzel, W.P., et al., 1998. Discriminating Clear Sky from Clouds with MODIS. *Journal of Geophysical Research: Atmospheres*. 103, 32141–32157. DOI: <https://doi.org/10.1029/1998JD200032>

[33] King, M.D., Menzel, W.P., Kaufman, Y.J., et al., 2003. Cloud and Aerosol Properties, Precipitable Water, and Profiles of Temperature and Water Vapor from MODIS. *IEEE Transactions on Geoscience and Remote Sensing*. 41, 442–458. DOI: <https://doi.org/10.1109/TGRS.2002.808226>

[34] Platnick, S., King, M., Ackerman, S.A., et al., 2003. The MODIS Cloud Products: Algorithms and Examples from Terra. *IEEE Transactions on Geoscience and Remote Sensing*. 41, 459–473. DOI: <https://doi.org/10.1109/TGRS.2002.808301>

[35] Georgoulias, A.K., Zanis, P., Pöschl, U., et al., 2013. QUantifying the Aerosol Direct and Indirect Effect over Eastern Mediterranean from Satellites (QUADIEEMS): Overview and Preliminary Results. *EGU General As-*

sembly Conference Abstracts. pp. EGU2013-1348

[36] Herman, J.R., Bhartia, P.K., Torres, O., et al., 1997. Global Distribution of UV-Absorbing Aerosols from Nimbus 7/TOMS Data. *Journal of Geophysical Research: Atmospheres*. 102, 16911–16922. DOI: <https://doi.org/10.1029/96jd03680>

[37] Levelt, P.F., van den Oord, G.H.J., Dobber, M.R., et al., 2006. The Ozone Monitoring Instrument. *IEEE Transactions on Geoscience and Remote Sensing*. 44, 1093–1101. DOI: <https://doi.org/10.1109/TGRS.2006.872333>

[38] Benedetti, A., Morcrette, J.J., Boucher, O., et al., 2009. Aerosol Analysis and Forecast in the European Centre for Medium-Range Weather Forecasts Integrated Forecast System: 2. Data Assimilation. *Journal of Geophysical Research: Atmospheres*. 114, 1–18. DOI: <https://doi.org/10.1029/2008JD011115>

[39] Dee, D.P., Uppala, S.M., Simmons, A.J., et al., 2011. The ERA-Interim Reanalysis: Configuration and Performance of the Data Assimilation System. *Quarterly Journal of the Royal Meteorological Society*. 137, 553–597. DOI: <https://doi.org/10.1002/qj.828>

[40] Mangold, A., De Backer, H., De Paepe, B., et al., 2011. Aerosol Analysis and Forecast in the European Centre for Medium-Range Weather Forecasts Integrated Forecast System: 3. Evaluation by Means of Case Studies. *Journal of Geophysical Research: Atmospheres*. 116, 1–23. DOI: <https://doi.org/10.1029/2010JD014864>

[41] Chin, M., Rood, R.B., Lin, S.J., et al., 2000. Atmospheric Sulfur Cycle Simulated in the Global Model GOCART: Model Description and Global Properties. *Journal of Geophysical Research: Atmospheres*. 105, 24671–24687. DOI: <https://doi.org/10.1029/2000JD900384>

[42] Gryspenert, E., Stier, P., Partridge, D.G., 2014. Satellite Observations of Cloud Regime Development: The Role of Aerosol Processes. *Atmospheric Chemistry and Physics*. 14, 1141–1158. DOI: <https://doi.org/10.5194/acp-14-1141-2014>

[43] Costantino, L., Bréon, F.M., 2013. Aerosol Indirect Effect on Warm Clouds over South-East Atlantic, from Co-Located MODIS and CALIPSO Observations. *Atmospheric Chemistry and Physics*. 13, 69–88. DOI: <https://doi.org/10.5194/acp-13-69-2013>

[44] Ghan, S.J., Guzman, G., Abdul-Razzak, H., 1998. Competition between Sea Salt and Sulfate Particles as Cloud Condensation Nuclei. *Journal of the Atmospheric Sciences*. 55, 3340–3347. DOI: [https://doi.org/10.1175/1520-0469\(1998\)055<3340:CBSSAS>2.0.CO;2](https://doi.org/10.1175/1520-0469(1998)055<3340:CBSSAS>2.0.CO;2)

[45] Feingold, G., Remer, L.A., Ramaprasad, J., et al., 2001. Analysis of Smoke Impact on Clouds in Brazilian Biomass Burning Regions: An Extension of Twomey's Approach. *Journal of Geophysical Research*. 106, 22907. DOI: <https://doi.org/10.1029/2001JD000732>

[46] Peng, J., Li, Z., Zhang, H., et al., 2016. Systematic Changes in Cloud Radiative Forcing with Aerosol Loading for Deep Clouds in the Tropics. *Journal of the Atmospheric Sciences*. 73, 231–249. DOI: <https://doi.org/10.1175/JAS-D-15-0080.1>

[47] Khain, A., Rosenfeld, D., Pokrovsky, A., 2005. Aerosol Impact on the Dynamics and Microphysics of Deep Convective Clouds. *Quarterly Journal of the Royal Meteorological Society*. 131, 2639–2663. DOI: <https://doi.org/10.1256/qj.04.62>

[48] Rosenfeld, D., Lohmann, U., Raga, G.B., et al., 2008. Flood or Drought: How Do Aerosols Affect Precipitation? *Science* (80). 321, 1309–1313. DOI: <https://doi.org/10.1126/science.1160606>

[49] Alexandri, G., Georgoulis, A.K., Meleti, C., et al., 2017. A High Resolution Satellite View of Surface Solar Radiation over the Climatically Sensitive Region of Eastern Mediterranean. *Atmospheric Research*. 188, 107–121. DOI: <https://doi.org/10.1016/j.atmosres.2016.12.015>

[50] Livingston, J.M., Russell, P.B., Reid, J.S., et al., 2003. Airborne Sun Photometer Measurements of Aerosol Optical Depth and Columnar Water Vapor during the Puerto Rico Dust Experiment and Comparison with Land, Aircraft, and Satellite Measurements. *Journal of Geophysical Research*. 108, 8588. DOI: <https://doi.org/10.1029/2002JD002520>

[51] Jin, M., Shepherd, J.M., 2008. Aerosol Relationships to Warm Season Clouds and Rainfall at Monthly Scales over East China: Urban Land versus Ocean. *Journal of Geophysical Research*. 113, D24S90. DOI: <https://doi.org/10.1029/2008JD010276>

[52] Tao, W.K., Chen, J.P., Li, Z., et al., 2012. Impact of Aerosols on Convective Clouds and Precipitation. *Reviews of Geophysics*. 50. DOI: <https://doi.org/10.1029/2011RG000369>

[53] Wang, F., Guo, J., Zhang, J., et al., 2015. Multi-Sensor Quantification of Aerosol-Induced Variability in Warm Clouds over Eastern China. *Atmospheric Environment*. 113, 1–9. DOI: <https://doi.org/10.1016/j.atmosenv.2015.04.063>

[54] Alam, K., Khan, R., Blaschke, T., et al., 2014. Variability of Aerosol Optical Depth and Their Impact on Cloud Properties in Pakistan. *Journal of Atmospheric and Solar-Terrestrial Physics*. 107, 104–112. DOI: <https://doi.org/10.1016/j.jastp.2013.11.012>

[55] Tripathi, S.N., Pattnaik, A., Dey, S., 2007. Aerosol Indirect Effect over Indo-Gangetic Plain. *Atmospheric Environment*. 41, 7037–7047. DOI: <https://doi.org/10.1016/j.atmosenv.2007.05.007>

[56] Saponaro, G., Kolmonen, P., Sogacheva, L., et al., 2017. Estimates of the Aerosol Indirect Effect over the Baltic Sea Region Derived from 12 Years of MODIS Observations. *Atmospheric Chemistry and Physics*. 17, 3133–3143. DOI: <https://doi.org/10.5194/acp-17-3133-2017>

[57] Fan, J., Yuan, T., Comstock, J.M., et al., 2009. Dominant Role by Vertical Wind Shear in Regulating Aerosol Effects on Deep Convective Clouds. *Journal of Geophysical Research: Atmospheres*. 114. DOI: <https://doi.org/10.1029/2009JD012352>

[58] Ten Hoeve, J.E., Remer, L.A., Jacobson, M.Z., 2011. Microphysical and Radiative Effects of Aerosols on Warm Clouds during the Amazon Biomass Burning Season as Observed by MODIS: Impacts of Water Vapor and Land Cover. *Atmospheric Chemistry and Physics*. 11, 3021–3036. DOI: <https://doi.org/10.5194/acp-11-3021-2011>

[59] Myhre, G., Stordal, F., Johnsrud, M., et al., 2007. Aerosol-Cloud Interaction Inferred from MODIS Satellite Data and Global Aerosol Models. *Atmospheric Chemistry and Physics*. 7, 3081–3101. DOI: <https://doi.org/10.5194/acp-7-3081-2007>

[60] Small, J.D., Jiang, J.H., Su, H., et al., 2011. Relationship between Aerosol and Cloud Fraction over Australia. *Geophysical Research Letters*. 38, 1–7. DOI: <https://doi.org/10.1029/2011GL049404>

[61] Yang, Q., Gustafson, W.I., Fast, J.D., et al., 2012. Impact of Natural and Anthropogenic Aerosols on Stratocumulus and Precipitation in the Southeast Pacific: A Regional Modelling Study Using WRF-Chem. *Atmospheric Chemistry and Physics*. 12, 8777–8796. DOI: <https://doi.org/10.5194/acp-12-8777-2012>

[62] Boreddy, S.K.R., Kawamura, K., Haque, M.M., 2015. Long-Term (2001–2012) Observation of the Modeled Hygroscopic Growth Factor of Remote Marine TSP Aerosols over the Western North Pacific: Impact of Long-Range Transport of Pollutants and Their Mixing States. *Physical Chemistry Chemical Physics*. 17, 29344–29353. DOI: <https://doi.org/10.1039/C5CP05315C>

[63] Titos, G., Burgos, M.A., Zieger, P., et al., 2021. A Global Study of Hygroscopicity-Driven Light-Scattering Enhancement in the Context of Other in Situ Aerosol Optical Properties. *Atmospheric Chemistry and Physics*. 21, 13031–13050. DOI: <https://doi.org/10.5194/acp-21-13031-2021>

[64] Remer, L.A., Tanré, D., Kaufman, Y.J., et al., 2002. Validation of MODIS Aerosol Retrieval over Ocean. *Geophysical Research Letters*. 29, MOD3-1–MOD3-4. DOI: <https://doi.org/10.1029/2001GL013204>

[65] Bellouin, N., Quaas, J., Morcrette, J.J., et al., 2013. Estimates of Aerosol Radiative Forcing from the MACC Re-Analysis. *Atmospheric Chemistry and Physics*. 13, 2045–2062. DOI: <https://doi.org/10.5194/acp-13-2045-2062>